applied microbiology

MDPI

Review

Asteltoxins: Synthesis and Biological Studies

Eslam R. El-Sawy [1], Gilbert Kirsch [2] and Mohamed S. Abdel-Aziz [3,*]

[1] Chemistry of Natural Compounds Department, National Research Centre, Giza 12622, Egypt; eslamelsawy@gmail.com
[2] Laboratoire Lorrain de Chimie Moléculaire (L.2.C.M.), Université de Lorraine, 57050 Metz, France; gilbert.kirsch@univ-lorraine.fr
[3] Microbial Chemistry Department, Biotechnology Research Institute, National Research Centre, Giza 12622, Egypt
* Correspondence: mohabomerna@yahoo.ca

Abstract: Asteltoxins belong to a group of polyene pyrone mycotoxins that are known to be potent inhibitors of mitochondrial ATP synthesis and ATP hydrolysis. Asteltoxin A was first isolated from the toxic maize cultures of *Aspergillus stellatus*. Several attempts have been made to synthesize asteltoxin A, starting with the synthesis of a bis(tetrahydrofuran) moiety that has been demonstrated previously in biosynthetic studies. This review highlights the fungal sources of asteltoxins, similar asteltoxins, biosynthetic pathways, their synthetic trials, and their biological activities. This review is the first of its kind covering the periods from 1979 to 2023.

Keywords: asteltoxins; sources; biosynthesis; synthesis; biological activity

check for updates

Citation: El-Sawy, E.R.; Kirsch, G.; Abdel-Aziz, M.S. Asteltoxins: Synthesis and Biological Studies. *Appl. Microbiol.* **2023**, *3*, 592–604. https://doi.org/10.3390/applmicrobiol3030042

Academic Editor: Ian Connerton

Received: 8 June 2023
Revised: 17 June 2023
Accepted: 19 June 2023
Published: 21 June 2023

1. Introduction

Mycotoxins are secondary metabolites produced by fungi capable of causing disease and death in humans and animals [1]. There have been many different mycotoxins discovered, but the most prevalent mycotoxins that are harmful to both humans and animals are aflatoxins, ochratoxin A, patulin, fumonisins, zearalenone, and nivalenol/deoxynivalenol. When crops are infected with mold before and after harvest, mycotoxins enter the food chain. Mycotoxins can be ingested directly through contaminated food or indirectly through consuming animals fed contaminated feed [1]. Some mycotoxin derivatives have exceptional biological activity and are used as antibiotics (penicillin and citrinin) [2], to relieve migraine attacks (ergotamine) [2] and as plant growth stimulants (*Fusarium* metabolites) [3].

Asteltoxins are mycotoxins belonging to a structural group featuring an α-pyrone attached to a 2, 8-dioxabicyclo [3.3.0] octane ring via a triene linker [4] and that are structurally related to citreoviridin and aurovertin [5], except for asteltoxin G which contains a tetrahydrofuran ring instead of a 2, 8-dioxabicyclo [3.3.0] octane ring [6] (Figure 1).

Asteltoxin A (**1**) has been isolated from the toxic maize meal cultures of *Aspergillus stellatus* Curzi (MRC 277) [7,8]. Asteltoxin A (**1**) was also isolated from *Emericella variecolor* [9]. Asteltoxin A (**1**) was the first identified member of the asteltoxins, which was isolated and chemically elucidated via spectroscopic methods and single-crystal X-ray analysis as mentioned by Rabie and his coworkers [7].

Other asteltoxin families such as asteltoxins B (**2**), C (**3**), and D (**4**) were produced by *Pochonia bulbillosa* 8-H-28 [10], whereas asteltoxins E (**5**) and F (**6**) were purified from *Aspergillus* sp. SCSIO XWS02F40 [11], and asteltoxin G (**7**) was obtained from *Aspergillus ochraceopetaliformis* [12]. Additionally, asteltoxin H (**8**) was isolated from the fungus *Pochonia suchlasporia* var. *suchlasporia* TAMA 87 [6] (Figure 1).

On the other hand, asteltoxins were reported to be isolated as secondary metabolites of *Aspergillus karnatakaensis* [13], *Aspergillus aeneus* [13], *Aspergillus terreus* [14], and *Aspergillus alabamensis* [14].

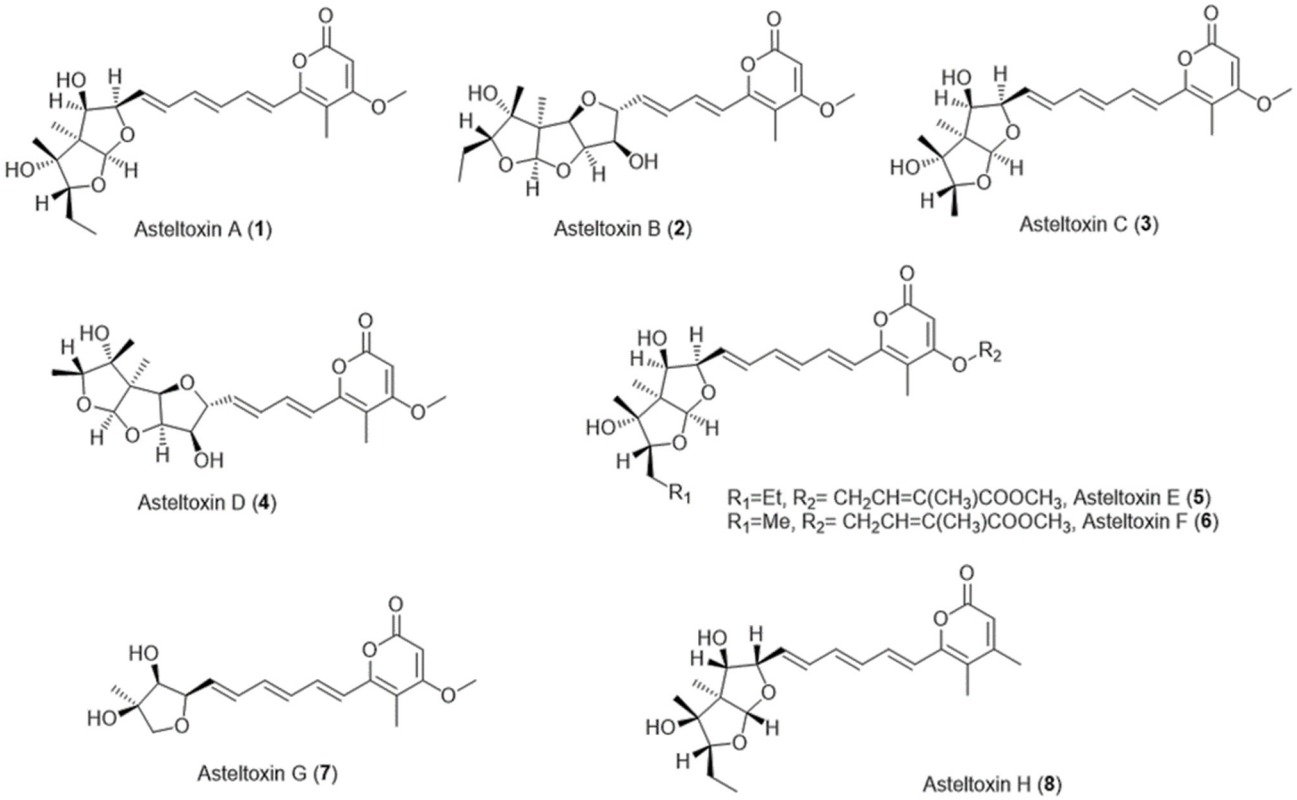

Figure 1. Chemical structures of asteltoxins A–H.

The chemical backbones of the natural asteltoxins A-G share the same α-pyrone moiety (4-methoxy-5-methyl-2-pyrone-based structure), but asteltoxin H has another type of α-pyrone moiety (3, 5-dimethyl-2-pyrone-based structure) (Figure 1).

Bao et al. (2013) [15] and Wu et al. (2015) [16] isolated an analog of asteltoxin A (**1**) from the gorgonian-derived fungus *Aspergillus* sp. SCSGAF 0076 and a sponge-associated fungus *E. variecolor*, respectively. They identified this analog as asteltoxin B with an epoxy group at C-7/C-8, which contradicts the known chemical form of the known asteltoxin B. They chemically elucidated its structure by spectroscopy, including affinities for ^{1}H-^{1}H COZY, HMBC, and NOESY.

Interestingly, similar asteltoxins have been identified that include asteltoxin-bearing dimers and prenylated asteltoxins (Figure 2).

Three novel asteltoxin-bearing dimers, named diasteltoxins A−C (**9**–**11**) (Figure 2), were isolated from a mutated strain of a sponge-derived fungus *Emericella variecolor* XSA-07-2 [17]. Four new prenylated asteltoxin derivatives, named avertoxins A (**12**), B (**13**), C (**14**), and D (**15**) (O-prenyl and C-prenyl asteltoxins) (Figure 2), were isolated from *Aspergillus versicolor* Y10, an endophytic fungus isolated from *Huperzia serrata* [18].

Asteltoxin A (**1**) possesses a range of biological activities, including potent inhibition against bacterial ATP synthesis and ATP hydrolysis catalyzed by mitochondrial enzyme systems [19]. On the other hand, asteltoxin and its similar compounds showed various biological activities, viz., antiviral [11], antiproliferative [10], and insecticidal [6] activities, as well as human acetylcholinesterase inhibition [18].

Evidence suggests that the bis(tetrahydrofuran) moiety is responsible for the inhibition and binding properties of asteltoxins [8].

The present review describes the different sources of asteltoxins, their biosynthetic and synthetic pathways, as well as their biological activities for the first time.

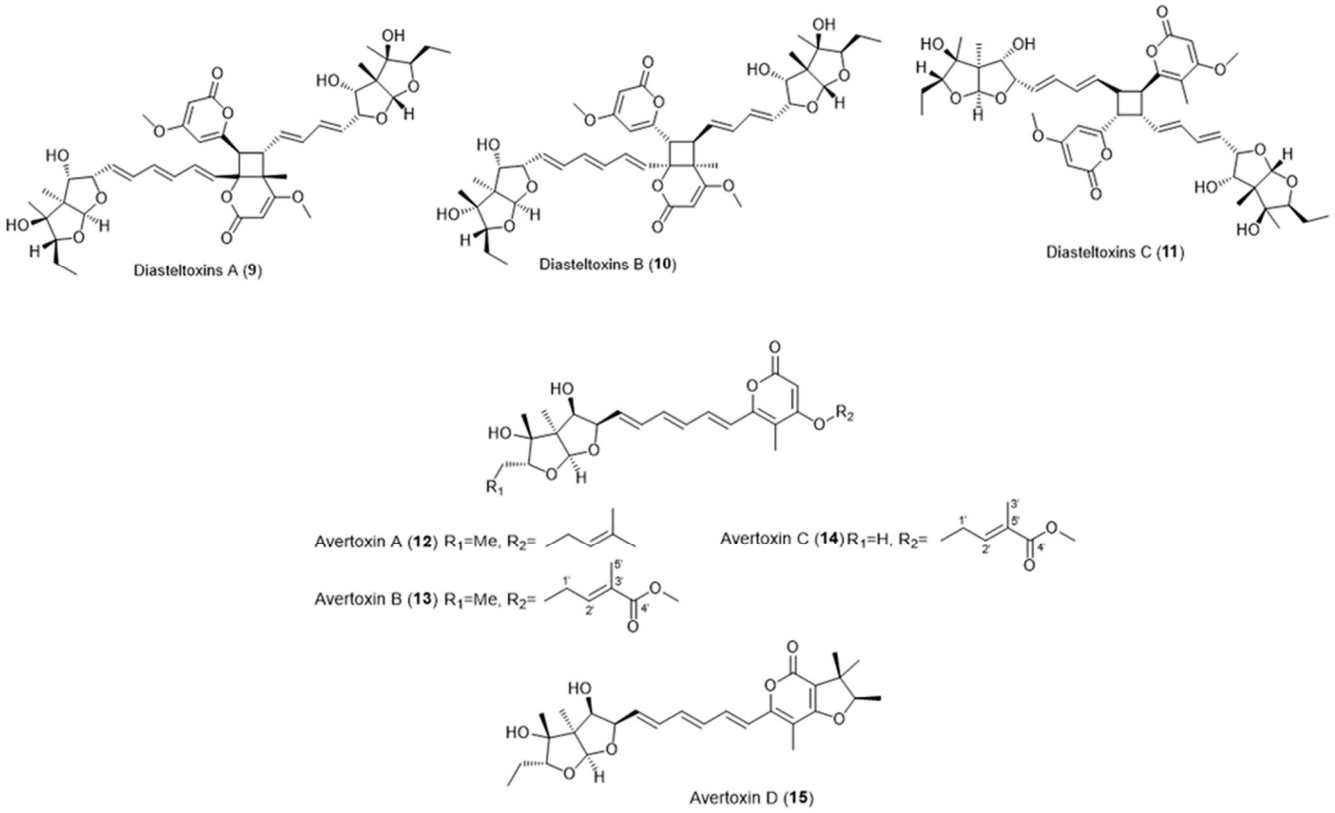

Figure 2. Chemical structures of similar asteltoxins. Diasteltoxin A (**9**), Diasteltoxin B (**10**), Disasteltoxin C (**11**), Avertoxin A (**12**), Avertoxin B (**13**), Avertoxin C (**14**), and Avertoxin D (**15**).

2. Biosynthesis

Vleggaar estimated the biosynthesis of asteltoxin A (**1**) through the polyepoxidation of a linear polyene precursor using ^{13}C and ^{18}O labeling experiments. His hypothesis was based on the formation of a diatomic moiety, bis(tetrahydrofuran) (**21**), by converting a 1,2-alkyl epoxide (**17**) from a polyketide chain (**16**) to generate a branched aldehyde that can be used in the total synthesis of asteltoxin A (Scheme 1) [20–22].

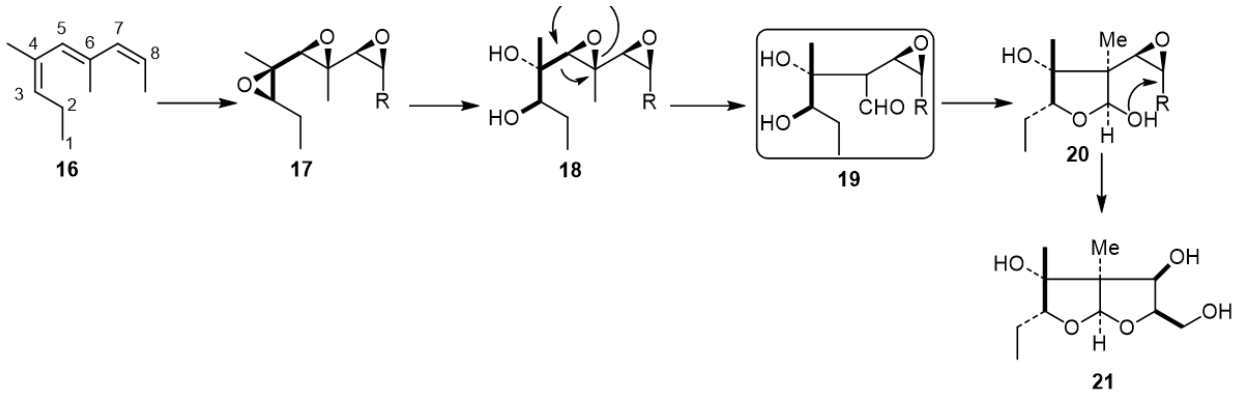

Scheme 1. Postulated biosynthesis of 2,8-dioxabicyclo[3.3.0]octane, (2S,3R,3aR,4R,6aR)-5-ethyl-3a,4-dimethylhexahydrofuro[2,3-b]furan-2,3,4-triol of the asteltoxins.

Recently, Mao and his coworkers identified two novel semi-pinacolases (SPases) AstD/MrvD that belong to the epoxide hydrolase (EH) family from the biosynthetic pathway of the fungal polyketide-type mycotoxin asteltoxin A (**1**) [23]. AstD/MrvD are bifunctional enzymes, working as EHs for region-selective epoxide ring opening on the bis-epoxide, and subsequently as SPases on the epoxy alcohol intermediate due to struc-

tural complexity. These two enzymes catalyzed the type III semi-pinacol rearrangement, (III SPR) for 2,3-migration. Also, these enzymes can recognize epoxy alcohol and catalyze the rearrangement of the polyketide backbone in C4 → C6 migration (Scheme 2). The *ast* gene cluster responsible for asteltoxin biosynthesis was first identified in *Emericella variecolor* NHL 2881 (Figure 3). These gene clusters were responsible for the SPase activity [23].

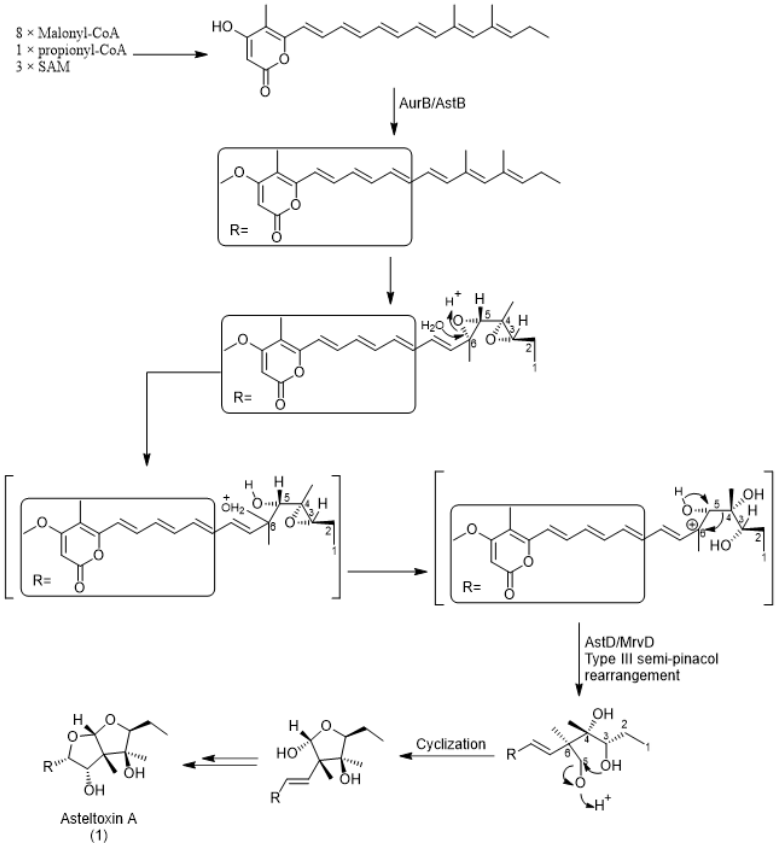

Scheme 2. Postulated biosynthesis of asteltoxin (**1**) based on two semi-pinacolases AstD/MrvD. 8 × Malonyl-CoA: coenzyme A derivative of malonic acid (eight units); 1 × propionyl-CoA: coenzyme A derivative of propionic acid (one unit); 3 × SAM: S-adenosyl methionine (three units).

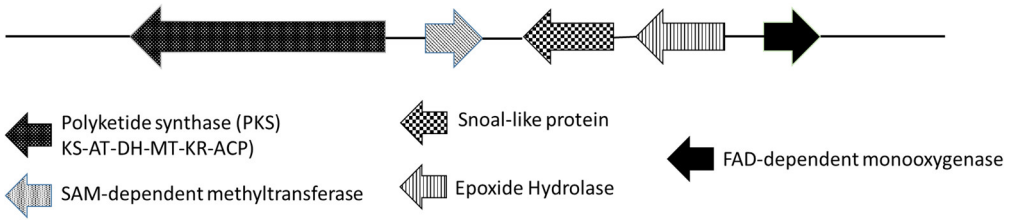

Figure 3. Gene clusters of asteltoxin A (**1**) from *E. variecolor*.

3. Stereochemistry

Vleggaar studied the biosynthetic origin of the carbon skeleton of asteltoxin by incorporating ^{13}C-labeled precursors: [1-^{13}C]propionate, (2*S*)-[methyl-^{13}C]methionine, and [1,2-$^{13}C_2$]acetate in addition to [1-^{13}C,$^{18}O_2$]acetate. He revealed the concurrent operation of two apparently free processes (A and B) in asteltoxin biosynthesis, taking into consideration the stereochemistry that occurred during the biosynthesis process [20,22].

Pathway (A) includes the methylation of the terminal C20-polyketide, with the consequent loss of the chain-initiating acetate group. Pathway (B) comprises a polyketide precursor that came from a propionate chain-initiating unit in addition to eight malonate units. The arrangement of entire acetate units in asteltoxin, which is derived from [1,2-

$^{13}C_2$]acetate, ensures that a 1,2-bond migration occurs during the formation of the 2,8-dioxabicyclo[3.3.0]octane moiety [20,22].

In detail, the ^{13}C-NMR spectrum of asteltoxin that came from [l—^{13}C]acetate revealed 9 signals attributed to the carbon numbers C-3, C-5, C-7, C-9, C-11,C-13, C-15, C-17, and -19. The NMR spectrum of asteltoxin that came from [2—^{13}C]acetate exhibited enhanced signals distinguished by carbon numbers C-2, C-4, C-6, C-8, C-10, C-12, C-14, C-16, and C-18. These results proved that the nine acetate units were involved in the formation of the metabolite. The positioning of the whole acetate units in asteltoxin was investigated by the addition of [l,2-$^{13}C_2$]acetate to cultures of *E. variecolor* [20].

The enriched asteltoxin exhibited multiple labeling (C-C) couplings between carbon atoms withdrawn from adjacent acetate units (inter-acetate coupling) depending on the proton-decoupled ^{13}C-NMR spectrum, along with the expected spin–spin coupling between carbon atoms that occurs with intact acetate units (intra-acetate coupling). The ^1J(CC) results of these couplings showed the existence of eight entire acetate units, organized as shown in Figure 4 [20].

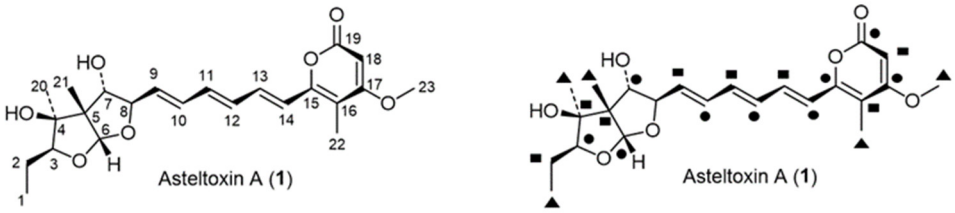

Figure 4. ^{13}C-labeling pattern for asteltoxin A (**1**), arrangement of intact acetate units in asteltoxin A (**1**). ▲(2*S*)-[methyl-^{13}C]-methionine; ■ = C-1 of acetate; ● = C-2 of acetate.

The previous results indicated that a 1,2-carbon C-4 shift eventually occurred in asteltoxin from C5 to C6 during biosynthesis, where a 1,2-bond migrated to an intact acetate unit and resulted in the slashing of a pinacol or epoxide rearrangement to provide a branched aldehyde that was subsequently utilized in the formation of the 2,8-dioxabicyclo[3.3.0]octane moiety (Scheme 1).

The incorporation of [2-^{13}C]acetate into asteltoxin revealed a number of resonances with low intensity signals due to one-bond (C, C) coupling. The presence of eight entire acetate units having an arrangement similar to that found in [1,2-$^{13}C_2$]acetate-derived asteltoxin has been studied through the analysis of the one-bond (C, C) coupling constants. Additionally, the ^{13}C-NMR spectrum demonstrated one-bond inter-acetate ^1JCC, which showed the presence of eight complete acetate units with an order corresponding to that found in [1,2-$^{13}C_2$]acetate-enriched asteltoxin. On the other hand, the ^{13}C-NMR spectrum also revealed one-bond inter-acetate ^1JCC due to the existence of carbon-4 (38.3 Hz) and carbon-5 (35.4 Hz), which may arise from couplings in each case with carbon-6. It is obvious that some of the [l,2-^{13}C2]acetate was formed through fermentation by the repeated recycling of [2-^{13}C]acetate in the Krebs citric acid cycle (pathway A)[20].

The addition of [1-^{14}C]propionate, with a specific activity of 11.29 μCi mmol^{-1} for 430 mg, to the cultures of *E. variecolor* to give asteltoxin with a specific activity of 0.76 μCi mmol^{-1} (26 mg) indicated the role of propionate in the biosynthesis of asteltoxin (pathway B) [20].

To investigate the mechanism of the 1,2-transformation that occurs in the context of biosynthesis and the stereochemistry of the intermediate transitions that lead to the structure of asteltoxin (Scheme 1), defining the origin of the oxygen atoms in the metabolite was needed [21]. Vleggaar and his coworkers designed an experimental study including sodium [l-13C,$^{18}O_2$]acetate (12.0 mmol) (50.6% $^{13}C^{18}O_2$, 41.0% $^{13}C^{18}O_2$, and 8.4% $^{13}C^{16}O$) admixed with sodium acetate (24.0 mmol), which was added to cultures of *Emericellu variecolor* [21]. The proton-decoupled ^{13}C NMR spectrum of the enriched asteltoxin showed ^{18}O-isotope shifts for the C-15, C-17, and C-19 resonances, indicating that the corresponding carbon–oxygen bonds had remained intact throughout the biosynthetic pathway. Addition-

ally, the disappearance of ^{18}O at either carbon-3, -5, or -7 (at resonances of 90.10, 112.98, and 80.19, respectively) showed the enhanced singlets. On the other hand, the deficiency of ^{18}O-labeling at carbon-4 and -8 predicted that these carbon atoms originated from C-2 of acetate.

The two novel β-ketolactones bearing polyenoic side chains in the asteltoxin compound aroused the interest of many scientists with regard to the mechanism of their formation inside the cell. Accordingly, several synthetic studies have been conducted to investigate this biosynthesis [24–27].

4. Chemical Synthesis

Asteltoxin A (**1**) has been a fascinating synthetic target for many scientific researchers. After biosynthetic studies of the bis(tetrahydrofuran) moiety of asteltoxin A by Vleggaar, there has been significant interest in the total synthesis of asteltoxin considering the preparation of a tetrahydrofuran ring.

The total synthesis of (±) asteltoxin A (**1**) was firstly accomplished by Schreiber and Satake in 1984 [28], which was followed by Tadano et al. in 1990 [29] and finally by Cha and his coworkers in 2003 [30].

Schreiber and Satake were the first researchers to prepare asteltoxin starting with 3,4-dimethylfuran (**22**) by going through sixteen steps with an overall yield of 3% (Scheme 3) [28,31–33].

In detail, the reaction starts with a Paternô–Buchi photocycloaddition of 3,4-dimethylfuran (**22**) and β-benzyloxypropanal (Scheme 3) [28]. Oxidation of the exo-substituted photoadduct (**23**) with *m*-chloro-per-benzoic acid (MCPBA) afforded the production of β-hydroxytetrahydrofuran (**24**). Hydrolysis of the latter compound created the corresponding *threo*-aldol as a monocyclic lactol, which was followed by protection with *N*,*N*-dimethylhydrazine to produce hydrazone (**25**). The chelation-controlled addition of ethyl magnesium bromide to compound (**25**) provided acetonide (**26**) after hydrolysis and internal protection. Deprotection of the benzyl ether, selenenylation, and selenoxide elimination followed by ozonolysis afforded the desired aldehyde (**27**). The reaction of the aldehyde (**27**) with Corey's anion (**29**) provided the pentadienyl sulfoxide (**30**) as a major stereoisomer compound. A Pummerer rearrangement and hydrolysis of (**30**) gave the corresponding aldehyde (**32**). The aldol condensation reaction of 32 with α-pyrone (**35**) yielded aldol product (**36**). Selective dehydration of the secondary hydroxyl on the side chain and tertiary hydroxyls on the ring provided (±) asteltoxin A (**1**) (Scheme 3). Asteltoxin A (**1**) was obtained as small pale-yellow needles, with an m.p. at 130–132 °C.

By comparing the sample of (±) asteltoxin A (**1**) that was obtained by this method with an authentic sample from nature, identical spectral and chromatographic properties were found; however, the sample existed as a racemic mixture.

Tadano et al. in 1990 reported an alternative synthetic pathway for the preparation of (±) asteltoxin A (**1**) starting from D-glucose (37) [24,29] (Scheme 4A): firstly the tetrahydrofuran (**38**) was obtained, which was converted and finally used to produce methyl glycoside (**44**) via multiple steps (ten steps in a row). The next challenge of their work was the introduction of cis-diol to the double bond in compound (**44**) [24]. Next, the cis-diol of compound (**44**) was turned into acetonide (**51**) through 10 consecutive steps (Scheme 4B). After three successive reactions including oxidation, reaction with triethyl 4-phosphonocrotonate (**53**), and acid hydrolysis, the bistetrahydrofuran (**54**) was obtained. The reduction of compound **54** followed by oxidation afforded the target aldehyde of Schreiber and Satake (**32**) [28]. Finally, aldehyde (**32**), under the same condition reaction of Schreiber and Satake with 4-methoxy-5,6-dimethyl-2*H*-pyran-2-one (**35**), gave (±) asteltoxin A (**1**) with a 73% yield (Scheme 4C) [29].

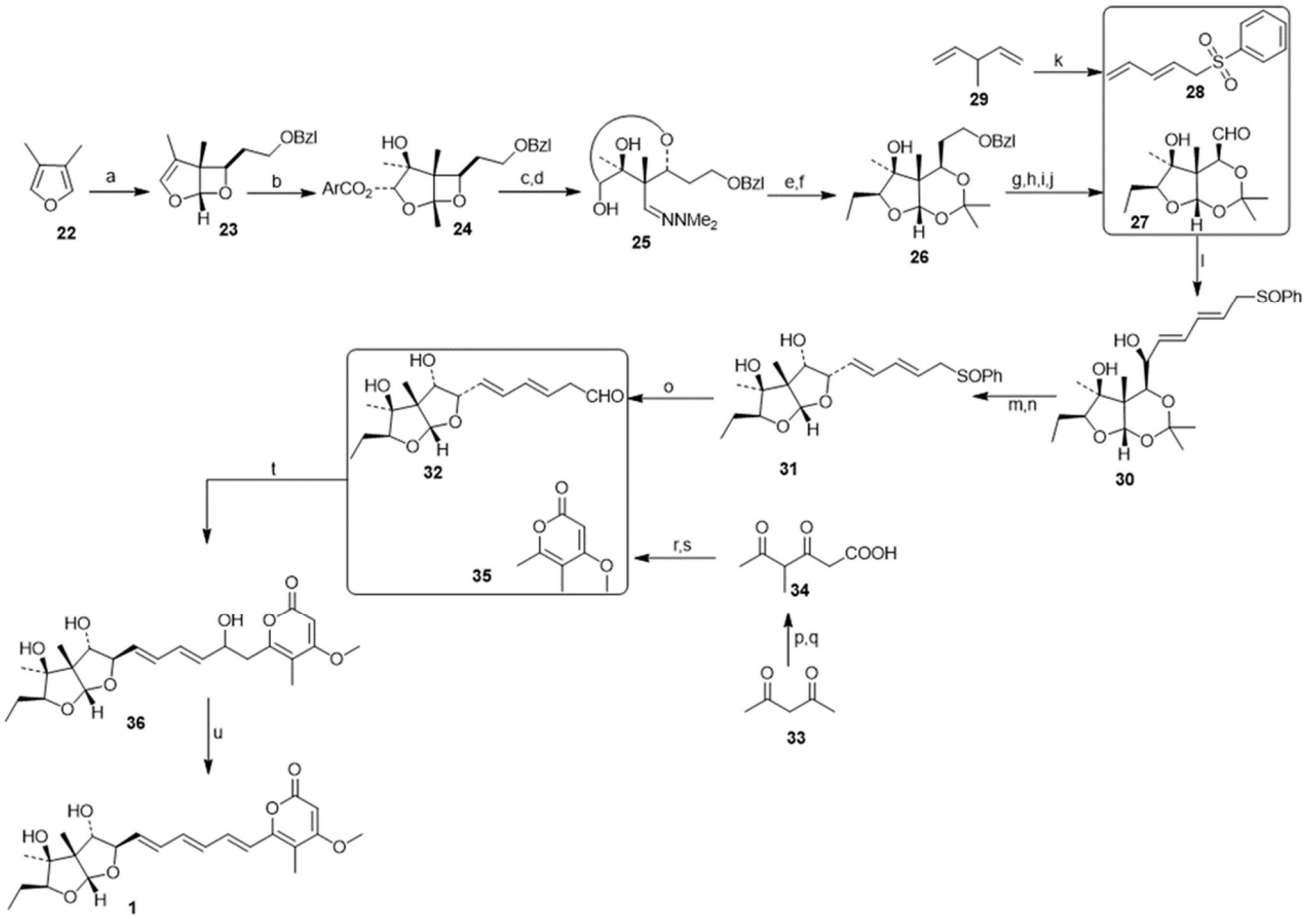

Scheme 3. Total synthesis of (±) asteltoxin A (**1**) via a Paternô–Buchi photocycloaddition of 3,4-dimethylfuran (**22**) and β-benzyloxypropanal. Reagents and conditions: (a) β-benzyloxypropanal, benzene, Et_2O, hυ (Vycor), 6 h, 63% yield; (b) *m*-chloro-per-benzoic acid (MCPBA), $NaHCO_3$, CH_2C1_2, 80% yield; (c) THF, HCl (3 N, 3:l); (d) $(Me)_2NNH_2$, CH_2CI_2, $MgSO_4$, 72% yield; (e) EtMgBr, THF, r.t., 48 h; (f) acetone, $CuSO_4$, camphorsulfonic acid (CSA), 55% yield; (g) Li, NH_3, Et_2O, 98% yield; (h) *o*-$NO_2C_6H_4SeCN$, Bu_3P_2, THF; (i) H_2O_2,THF, 81% yield; (j) O_3, CH_2Cl_2, MeOH, DMS, 92% yield; (k) *n*-BuLi, THF, −78 °C, PhSC1, −50 to 0 °C; (l) *n*-BuLi, THF, −78 °C; then, NH_4CI (aq), r.t., 3 h, 88% yield (3:l *β*/*α*); (m) CSA, CH_2Cl_2, 77% yield; (n) $CF_3CO_2COCH_3$, Ac_2O, 2,6,-lutidine; (o) $HgCI_2$, $CaCO_3$, CH_3CN, H_2O, 60% yield; (p) MeI, K_2CO_3, acetone; (q) $NaNH_2$, NH_3, Et_2O, CO_2; (r) (im)2CO, THF; (s) $(MeO)_2SO_2$, K_2CO_3, acetone; (t) lithium di-isopropyl amide (LDA), hexamethylphosphoramide (HMPA), THF, −78 °C, 80% yield; (u) TsCI, 4-dimethylaminopyridine (DMAP), Et_3N, CH_2Cl_2, 82% yield. (±) Asteltoxin A (**1**) overall yield was 3% through 16 steps.

In 2003, Cha and his coworkers achieved the synthesis of (±) asteltoxin A (**1**) via the Horner–Emmons olefination of bis(tetrahydrofuran) aldehyde and α-pyrone phosphonate [30].

They depended on the creation of a fully protected derivative of bis(tetrahydrofuran) core (**67**) through seventeen steps, starting with ethyl (*S*,*E*)-4,5-diisopropoxy-2-methylpent-2-enoate (**55**) (Scheme 5A). The straightforward sequence of functional group manipulation gave aldehyde (**69**), with a good overall yield (90%) starting with compound (**68**) (Scheme 5B). The condensation reaction of aldehyde (**69**) with α-pyrone phosphonate (**70**) in the presence of lithium bis(trimethylsilyl)amide (LiHMDS) achieved the derivative of bis(trimethylsilyl)-protected asteltoxin (**71**). The latter compound (**71**) was not protected by tetra-*n*-butylammonium fluoride (TBAF), which provided (±) asteltoxin A (**1**) with a 87–95% yield (Scheme 5B).

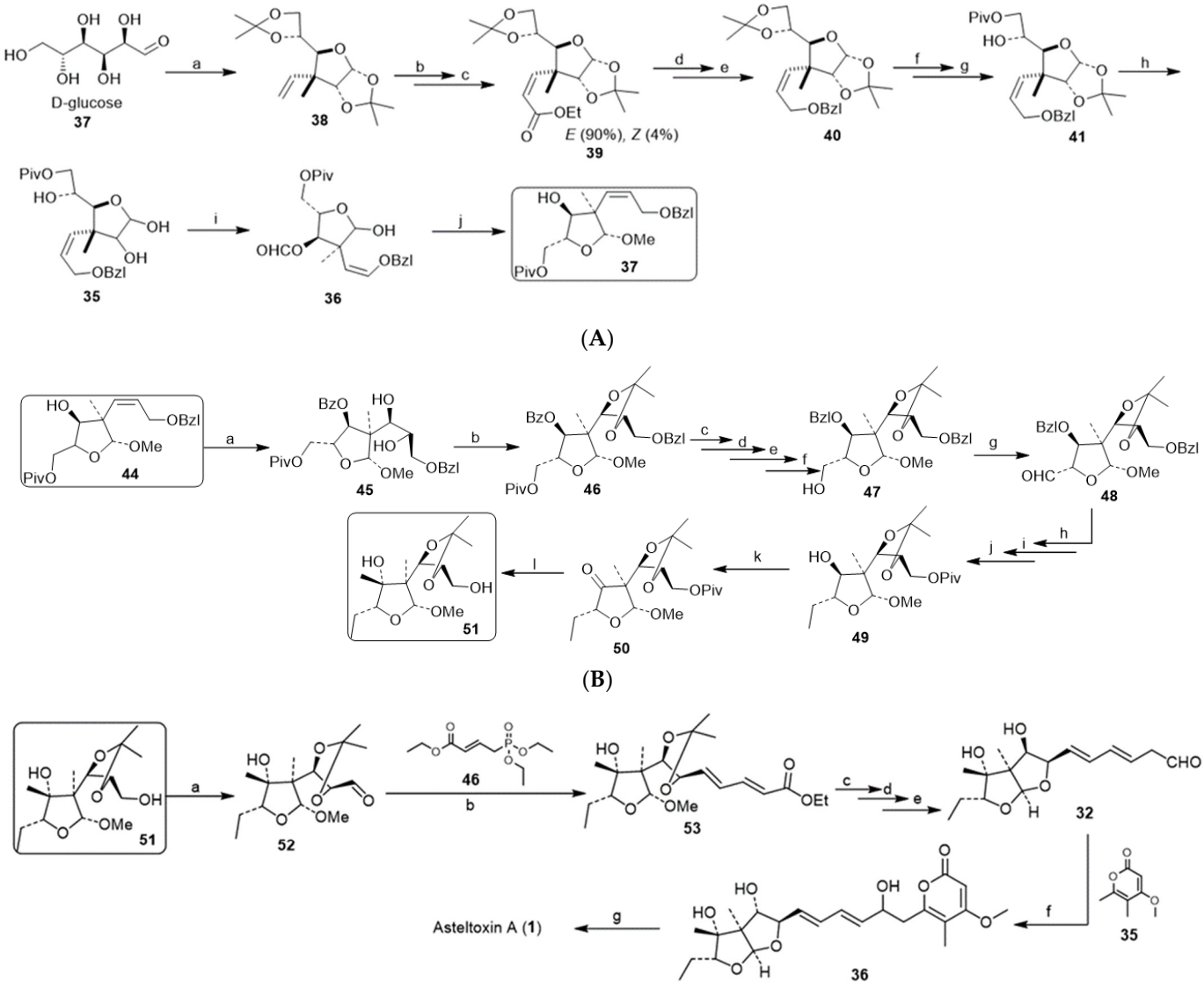

Scheme 4. (**A**) Synthetic pathway for the preparation of (±) asteltoxin A (**1**) starting from D-glucose. Reagents and conditions: (a) orthoester Claisen rearrangement; (b) i: O_3, CH_2Cl_2; ii: Ph_3P, (−78 °C to r.t.); (c) Ph_3P=CHCOOEt, benzene, reflux (*E* (90%): *Z* (4%) yields; (d) diisobutyl aluminum hydride (Dibal-H), CH_2Cl_2, −40 °C, 94% yield; (e) benzyl bromide, NaH, DMF, r.t.; (f) dil. AcOH (50%), r.t., 89% yield; (g) $Me_3CC(O)Cl$, pyridine, 4-dimethylaminopyridine (DMAP), CH_2Cl_2, r.t., 78% yield; (h) CF_3COOH (60%), 5 °C, 64 h; (i) $NaIO_4$, H_2O/MeOH, r.t.; (j) MeOH, Amberlite, reflux, 80% yield. (**B**) Reagents and conditions: (a) benzyl chloride, pyridine, 60C; (b) OSO_4, 2-methyl-2-propanol N-oxide (NMO), aq. acetone, r.t., 68% yield; (c) 2,2-dimethoxypropane, acetone, CSA, r.t.; (d) MeONa, MeOH, 0 °C, 90 min; (e) NaH, benzyl bromide, r.t., 62% yield; (f) DMF, r.t., 20 h, 83% yield; (g) i: DMSO, oxalyl chloride $(COCl)_2$, CH_2Cl_2, −78 °C, ii: Et_3N, −78 °C to r.t.; (h) i: $Ph3P^+MeBr^-$, $NaNH_2$, THF, reflux, ii: THF, r.t., 87% yield; (i) H_2, Raney Ni, EtOH, r.t., 4 days, 78% yield; (j) $Me_3CC(O)Cl$, pyridine, DMAP, CH2Cl2, r.t.; (k) PCC, MS, CH_2Cl_2, r.t.; (l) Me-MgBr, THF, 0 °C, 95% yield. (**C**) Reagents and conditions: (a) pyridinium chlorochromate (PCC), molecular sieves (MS), CH_2Cl_2, r.t.; (b) Wittig–Horner reaction, $(EtO)_2P(O)CH_2CH$=CHCOOEt, lithium di-isopropyl amide (LDA), THF, −78 °C; (ii) −78 °C to r.t., 72% yield; (c) CF_3COOH (60%), r.t., 89% yield; (d) Dibal-H, CH_2Cl_2, −78 °C, 78% yield; (e) MnO_2, CH_2Cl_2, r.t., 86% yield; (f) i: LDA, THF, HMP, −78 °C; ii: −78 °C, 15 min; (g) TScL, DMAP, Et_3N, CH_2Cl_2, r.t., 73% yield.

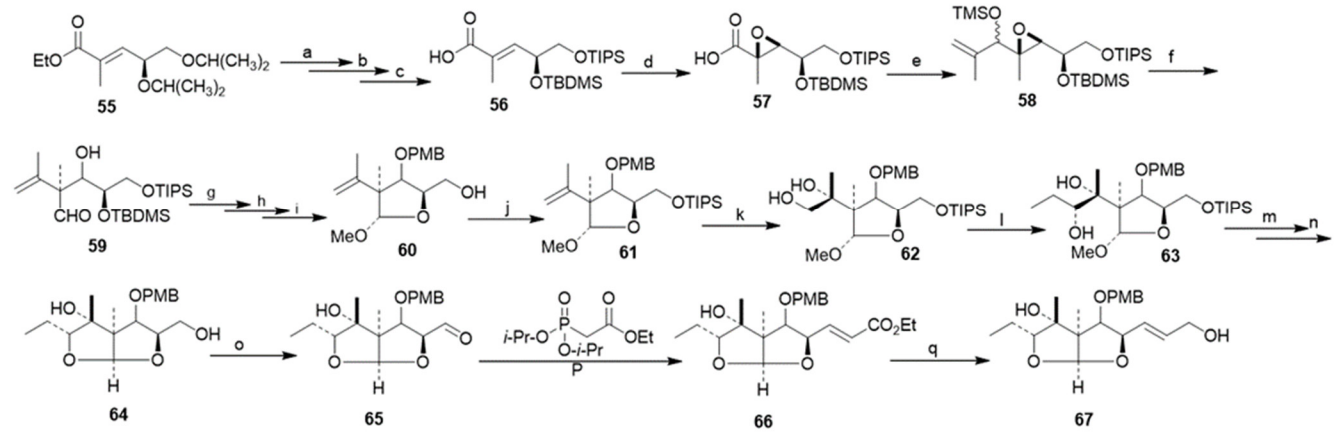

(**A**)

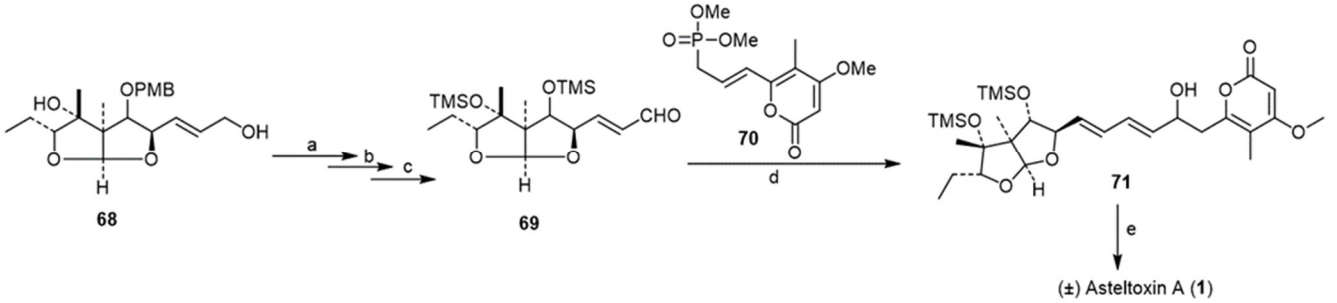

(**B**)

Scheme 5. (**A**) Synthetic pathway for the preparation of (±) asteltoxin A (**1**) starting from ethyl (*S*,*E*)-4,5-diisopropoxy-2-methylpent-2-enoate. Reagents and conditions: (a) 5% HCl, THF, 85% yield; (b) tert-butyldimethylsilyl trifluoromethanesulfonate (TBDMSOTf), tert-butyldimethylsilyl ether (TBDMS), 88% yield, (c) diisobutylaluminum (DIBAL) reduction, −78 °C, 90% yield; (d) i: diisopropyltryptamine (±) DIPT, molecular sieves (MS), CH_2Cl_2, −40 °C, Ti(O-*i*-Pr)$_4$, ii: tert-butyl hydroperoxide (TBHP, 2 M), CH_2Cl_2, −20 °C, 6 h, 80% yield; (e) i: tetrapropylammonium perruthenate (TPAP), r.t., stirring, 30 min, ii: propenylmagnesium bromide, THF, r.t., stirring, 30 min, iii: 2,6-lutidine, TBDMSOTf, −20 °C, stirring, 30 min, 99% yield; (f) $TiCl_4$, CH_2Cl_2, −78 °C, 20 min, 93%; (g) THF, 2,2-dimethyl-1,3-dioxolane, HCl (1M), 82% yield; (h) THF, *p*-methoxybenzyl chloride (PMBCl), KH, 82% yield; (i) i: tetrabutylammonium fluoride, THF, ii: MeOH, HCl (1M), r.t., stirring, 2 h; (j) imidazole, DMAP, CH_2Cl_2, triisopropylsilyl chloride (TIBSCl), 80% yield; (k) OsO4, *N*-methylmorpholine N-oxide (NMO), acetone-H_2O (1:2), r.t., stirring, 2 h, 85% yield; (l) i: CH_2Cl_2, oxalyl chloride, −76 °C, ii: ethylmagnesium bromide (EtMgBr), THF, stirring, 2 h, 68% yield; (m) *p*-TsOH, stirring, r.t., 1.5 h, 95% yield; (n) tetrabutylammonium fluoride, THF, stirring, 30 min, 90% yield, (o) DMSO, CH_2Cl_2, oxalyl chloride, −76 °C; (p) *t*-BuOK, (−20 °C to 0 °C), 2 h, stirring, 79% yield; (q) diisobutylaluminum hydride (DIBAL), CH_2Cl_2, −76 °C to 0 °C, 78% yield. (**B**) Synthetic pathway for the preparation of (±) asteltoxin A (**1**) via the Horner–Emmons olefination of bis(tetrahydrofuran) aldehyde and α-pyrone phosphonate. Reagents and conditions: (a) i: pyridine, Ac_2O, 4-(dimethylamino)pyridine, stirring, r.t., ii: CH_2Cl_2-H_2O, 2,3-dichloro-5,6-dicyano-1,4-benzoquinone (DDQ), stirring, overnight, r.t., 92% yield; (b) 2,6-lutidine, TBDMSOTf, CH_2Cl_2, −78 °C, stirring, 90% yield; (c) i: DIBAL, CH_2Cl_2, −78 °C, ii: MnO_2; (d)THF, −78 °C, LiHMDS, stirring, 5 h; (e) THF, tetrabutylammonium fluoride (1 M), 4 °C, 1.5 days, stirring, 87–95% yield.

5. Biological Activities

Asteltoxin A (**1**) was the most important of all known asteltoxins, as it showed various biological activities, which included inhibition of *Escherichia coli* BFI-ATPase activity, quorum sensing (QS) inhibitor, extracellular vesicle (EV) inhibitor, and antiviral activity.

Asteltoxin A (**1**) was found to inhibit *Escherichia coli* BFI-ATPase activity and can serve as a valuable fluorescent probe for mitochondrial F, bacterial BF, and ATPases [6]. Evidence suggests that the bis(tetrahydrofuran) moiety is responsible for the inhibition and binding properties of asteltoxin A [6].

Asteltoxin A (**1**), a respiratory toxin from *Emericella variecolor*, was examined to determine its inhibitory effect on mitochondrial function. Mitochondrial respiration is divided into different states, where each represents a different stage of oxygen consumption. State 3 of respiration represents oxygen consumption after ADP addition in the presence of a certain substrate, while state 4 represents oxygen consumption after ADP is completely transformed into ATP (i.e., in the absence of ADP). It was reported that the addition of asteltoxin (15 nmol) to mitochondria isolated from rat liver, before adding ADP and succinate, prevented state 3 and state 4 respiration processes. Hence, asteltoxin was shown to be able to inhibit the ATP synthesis system in mitochondria, leading to state 3 suppression; it was also found that asteltoxin A strongly decreases Mg2+-ATPase activity in mitochondria and slightly affects Na+- and K+-activated ATPases in microsomes at the concentration range for the inhibition of mitochondrial respiration [13]. This confirms that asteltoxin A (**1**) inhibits the energy transfer system in mitochondria, specifically inhibiting Mg2+-ATPase activity [13].

Asteltoxin A (**1**) is considered as a known quorum sensing (QS) inhibitor from the marine fungus Penicillium sp. QF046. It exhibits potent inhibition of violacein compared to the positive control, (Z-)-4-bromo-5-(bromomethylene)-2(5H)-furanone, meaning that it decreases the expression of multiple QS-related genes (*lasA*, *lasB*, *vioB*, *vioI*, *cynS*, and *hcnB*) [31].

Asteltoxin A (**1**) was represented as a new type of extracellular vesicle (EV) inhibitor that controls the fate of multi-vesicular bodies (MVBs). In detail, after treatment with asteltoxin at low concentrations (0.1, 1.0, and 10 µg/mL), the adenosine monophosphate/adenosine triphosphate (AMP/ATP) ratio increases due to the inhibition of ATP synthase, and this increase induces AMPK-mediated suppression of mTORC1. Inactivation of the mammalian target of rapamycin complex 1 (mTORC1) promotes nuclear translocation of the microphthalmia/transcription factor E (MiT/TFE) family members, thereby inducing transcription of lysosome-related genes and activation of the lysosomal function. MVBs are then degraded, and the number of MVBs fused with the plasma membrane is low, resulting in the suppression of EV secretion (Figure 5) [34].

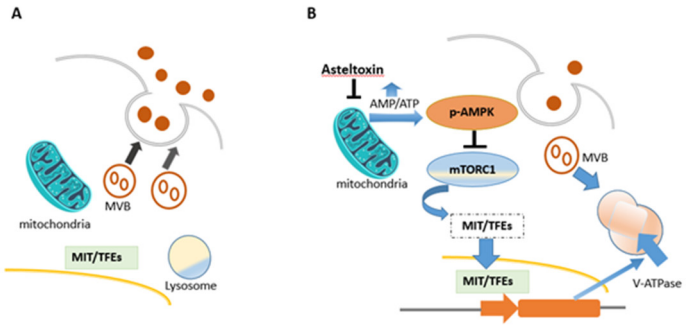

Figure 5. Schematic flowsheet considering the role of asteltoxin in regulating the fate of multi-vesicular bodies (MVBs) and regulation of EV secretion. (**A**) MVBs fuse with the plasma membrane and endorse EV secretion in cancer cells. (**B**) After asteltoxin A (**1**) treatment.

Asteltoxin A (**1**) and isoasteltoxin (Figure 6), which were isolated from the Antarctic soil-derived fungus *Aspergillus ochraceopetaliformis* SCSIO 05702, were reported to exhibit antiviral activities against the H1N1 and H3N2 influenza viruses with IC_{50} values of >0.54 ± 0.06/0.84 ± 0.02 and 0.23 ± 0.05/0.66 ± 0.09 µM, respectively [35,36].

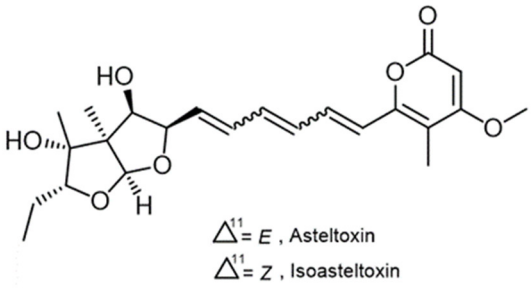

Figure 6. Chemical structures of asteltoxin A (**1**) and isoasteltoxin.

On the other hand, various biological activities have been registered by different asteltoxins and their similar compounds. The data in Table 1 summarize the different biological activities of asteltoxins and their similar compounds.

Table 1. Various biological activity of asteltoxins and their similar compounds.

Asteltoxin Compounds	Activity	Ref
Asteltoxin C (**3**)	Antiproliferative activity against NIAS-SL64 cells derived from the body fat of *Spodoptera litura larvae*.	[10]
Asteltoxin H (**8**)	Insecticidal activity against prepupae of the blowfly, *Lucilia sericata*, with an LD50 value of 0.94 μg/mg of prepupal body weight.	[6]
Asteltoxins E (**5**) and F (**6**)	Antiviral activity against H3N2 with the prominent IC_{50} values of 6.2 ± 0.08 and 8.9 ± 0.3 μM, respectively.	[11]
asteltoxin F (**6**)	Antiviral activity with inhibitory activity against H1N1 with an IC_{50} value of 3.5 ± 1.3 μM.	[11]
Diasteltoxins A-C (**66**–**68**)	Antiproliferative effects against H1299 (human lung cancer) and MCF7 (human breast cancer) cells. Applicable inhibition against thioredoxin reductase (TrxR) with IC_{50} 12.8 ± 0.8, 11.1 ± 0.2, and 7.2 ± 0.2 μM, respectively.	[17]
Avertoxin B (**70**)	Human acetylcholinesterase inhibition with the IC_{50} value of 14.9 μM.	[18]

6. Conclusions

Asteltoxins are a group of secondary metabolites belonging to fungal mycotoxins. They are known to be a group of polyene pyrone mycotoxins. They play a crucial role as an inhibitor against bacterial ATP synthesis and ATP hydrolysis. Several studies have been carried out to synthesize asteltoxin A (**1**) based on the biosynthetic pathway of the naturally occurring bis(tetrahydrofuran); thus the total synthesis of (±) asteltoxin A has been achieved. There have been many different asteltoxins discovered, asteltoxins featuring an α-pyrone attached to a 2, 8-dioxabicyclo [3.3.0] octane ring via a triene linker (asteltoxins A-H), besides asteltoxin-bearing dimers (diasteltoxins A−C) and prenylated asteltoxins (avertoxins A-D). Evidence indicates that the asteltoxins' inhibition and binding abilities are caused by the bis(tetrahydrofuran) moiety. Notably, asteltoxin A was chosen to investigate its inhibitory effect on mitochondrial function in various previous studies. So, we expect to use it to control the respiratory system in different pathogenic organisms including bacteria, fungi, and insects.

Author Contributions: Conceptualization, M.S.A.-A.; resources, G.K.; analysis and writing—original draft, E.R.E.-S.; writing—review and editing final draft, M.S.A.-A. and E.R.E.-S.; analysis with constructive discussion, M.S.A.-A. All authors have read and agreed to the published version of the manuscript.

Funding: This research received no external funding.

Data Availability Statement: Not applicable.

Acknowledgments: The authors are grateful to the National Research Center, Egypt, for allowing us to use their electronic facilities which led to the completion of the current work.

Conflicts of Interest: The authors declare no conflict of interest.

References

1. Bennett, J.W.; Klich, M. Mycotoxins. *Clin. Microbiol. Rev.* **2003**, *16*, 497–516. [CrossRef] [PubMed]
2. Omar, H.E.-D.M. Mycotoxins-Induced Oxidative Stress and Disease. In *Mycotoxin and Food Safety in Developing Countries*; IntechOpen: London, UK, 2013; ISBN 978-953-51-1096-5.
3. Bitas, V.; McCartney, N.; Li, N.; Demers, J.; Kim, J.-E.; Kim, H.-S.; Brown, K.M.; Kang, S. Fusarium Oxysporum Volatiles Enhance Plant Growth Via Affecting Auxin Transport and Signaling. *Front. Microbiol.* **2015**, *6*, 1248. [CrossRef] [PubMed]
4. Lin, T.-S.; Chiang, Y.-M.; Wang, C.C.C. Biosynthetic Pathway of the Reduced Polyketide Product Citreoviridin in Aspergillus Terreus Var. Aureus Revealed by Heterologous Expression in Aspergillus Nidulans. *Org. Lett.* **2016**, *18*, 1366–1369. [CrossRef] [PubMed]
5. Forbes, J.E.; Pattenden, G. Total Synthesis of Preaurovertin, Putative Biogenetic Precursor of Aurovertin. Biosynthetic Interrelationships between the Aurovertins, Citreoviridinols and Asteltoxin. *J. Chem. Soc. Perkin Trans. 1* **1991**, *8*, 1959–1966. [CrossRef]
6. Suminto, S.; Takatsuji, E.; Iguchi, A.; Kanzaki, H.; Okuda, T.; Nitoda, T. A New Asteltoxin Analog with Insecticidal Activity from Pochonia Suchlasporia TAMA 87. *J. Pestic. Sci.* **2020**, *45*, 81–85. [CrossRef]
7. Kruger, G.J.; Steyn, P.S.; Vleggaar, R.; Rabie, C.J. X-ray Crystal Structure of Asteltoxin, a Novel Mycotoxin from Aspergillus Stellatus Curzi. *J. Chem. Soc. Chem. Commun.* **1979**, *10*, 441–442. [CrossRef]
8. Satre, M. The Effect of Asteltoxin and Citreomontanine, Two Polyenic α-Pyrone Mycotoxins, on Escherichia Coli Adenosine Triphosphatase. *Biochem. Biophys. Res. Commun.* **1981**, *100*, 267–274. [CrossRef]
9. Frisvad, J.C.; Samson, R.A. Emericella Venezuelensis, a New Species with Stellate Ascospores Producing Sterigmatocystin and Aflatoxin B1. *Syst. Appl. Microbiol.* **2004**, *27*, 672–680. [CrossRef]
10. Adachi, H.; Doi, H.; Kasahara, Y.; Sawa, R.; Nakajima, K.; Kubota, Y.; Hosokawa, N.; Tateishi, K.; Nomoto, A. Asteltoxins from the Entomopathogenic Fungus Pochonia Bulbillosa 8-H-28. *J. Nat. Prod.* **2015**, *78*, 1730–1734. [CrossRef]
11. Tian, Y.-Q.; Lin, X.-P.; Wang, Z.; Zhou, X.-F.; Qin, X.-C.; Kaliyaperumal, K.; Zhang, T.-Y.; Tu, Z.-C.; Liu, Y. Asteltoxins with Antiviral Activities from the Marine Sponge-Derived Fungus Aspergillus Sp. SCSIO XWS02F40. *Molecules* **2016**, *21*, 34. [CrossRef]
12. Liu, J.-T.; Wu, W.; Cao, M.-J.; Yang, F.; Lin, H.-W. Trienic α-Pyrone and Ochratoxin Derivatives from a Sponge-Derived Fungus Aspergillus Ochraceopetaliformis. *Nat. Prod. Res.* **2018**, *32*, 1791–1797. [CrossRef] [PubMed]
13. Varga, J.; Frisvad, J.C.; Samson, R.A. Aspergillus Sect. Aeni Sect. Nov., a New Section of the Genus for A. Karnatakaensis Sp. Nov. and Some Allied Fungi. *IMA Fungus* **2010**, *1*, 197–205. [CrossRef] [PubMed]
14. Samson, R.A.; Peterson, S.W.; Frisvad, J.C.; Varga, J. New Species in Aspergillus Section Terrei. *Stud. Mycol.* **2011**, *69*, 39–55. [CrossRef] [PubMed]
15. Bao, J.; Zhang, X.-Y.; Xu, X.-Y.; He, F.; Nong, X.-H.; Qi, S.-H. New Cyclic Tetrapeptides and Asteltoxins from Gorgonian-Derived Fungus Aspergillus Sp. SCSGAF 0076. *Tetrahedron* **2013**, *69*, 2113–2117. [CrossRef]
16. Wu, Q.; Long, H.-L.; Liu, D.; Proksch, P.; Lin, W.-H. Varioxiranols I-L, New Lactones from a Sponge-Associated Emericella Variecolor Fungus. *J. Asian Nat. Prod. Res.* **2015**, *17*, 1137–1145. [CrossRef]
17. Long, H.; Cheng, Z.; Huang, W.; Wu, Q.; Li, X.; Cui, J.; Proksch, P.; Lin, W. Diasteltoxins A-C, Asteltoxin-Based Dimers from a Mutant of the Sponge-Associated Emericella Variecolor Fungus. *Org. Lett.* **2016**, *18*, 4678–4681. [CrossRef]
18. Wang, M.; Sun, M.; Hao, H.; Lu, C. Avertoxins A–D, Prenyl Asteltoxin Derivatives from Aspergillus Versicolor Y10, an Endophytic Fungus of Huperzia Serrata. *J. Nat. Prod.* **2015**, *78*, 3067–3070. [CrossRef]
19. Kawai, K.; Fukushima, H.; Nozawa, Y. Inhibition of Mitochondrial Respiration by Asteltoxin, a Respiratory Toxin from Emericella Variecolor. *Toxicol. Lett.* **1985**, *28*, 73–77. [CrossRef]
20. Steyn, P.S.; Vleggaar, R. Biosynthesis of Asteltoxin by Cultures of Emericella Variecolor. The Role of Propionate in the Biosynthesis and Evidence for a 1,Z-Bond Migration in the Formation of the Bistetrahydrofuran Moiety. *J. Chem. Soc. Chem. Commun.* **1984**, *15*, 977–979. [CrossRef]
21. de Jesus, A.E.; Steyn, P.S.; Vleggaar, R. Application of 18O Induced Isotope Effects in 13C n.m.r. Spectroscopy to the Biosynthesis of Asteltoxin. *J. Chem. Soc. Chem. Commun.* **1985**, *22*, 1633–1635. [CrossRef]
22. Vleggaar, R. Biosynthetic Studies on Some Polyene Mycotoxins. *Pure Appl. Chem.* **1986**, *58*, 239–256. [CrossRef]
23. Cao, F.; Tao, W.-T.; Yu, Q.; Xu, C.-X.; Cheng, J.-T.; Liu, R.-X.; Zhao, Q.-W.; Jiang, X.-H.; Liu, Y.; Li, Y.-Q.; et al. Discovery of Semi-Pinacolases from the Epoxide Hydrolase Family during Efficient Assembly of a Fungal Polyketide. *ACS Catal.* **2021**, *11*, 14702–14711. [CrossRef]
24. Tadano, K.; Yamada, H.; Idogaki, Y.; Ogawa, S.; Suami, T. Stereoselective Synthesis of the Bis(Tetrahydrofuran) Moiety (C-1 to C-9) of (+)-Asteltoxin, a Novel Mycotoxin from Aspergillus Stellatus. *Tetrahedron Lett.* **1988**, *29*, 655–658. [CrossRef]
25. Raman, J.V.; Lee, H.K.; Vleggaar, R.; Cha, J.K. A Formal Synthesis of (+)-Asteltoxin. *Tetrahedron Lett.* **1995**, *36*, 3095–3098. [CrossRef]

26. Mulzer, J.; Mohr, J.-T. Stereoselective Synthesis of the Bis-Tetrahydrofuran Fragment (C-1-C-9) of Asteltoxin. *J. Org. Chem.* **1994**, *59*, 1160–1165. [CrossRef]
27. Nishiyama, S.; Kanai, H.; Yamamura, S. Synthesis of Optically Active Hexahydrofuro[2,3- *b*]Furan, A Nonchromophore Moiety of Asteltoxin. *Bull. Chem. Soc. Jpn.* **1990**, *63*, 1322–1327. [CrossRef]
28. Schreiber, S.L.; Satake, K. Total Synthesis of (+-)-Asteltoxin. *J. Am. Chem. Soc.* **1984**, *106*, 4186–4188. [CrossRef]
29. Tadano, K.; Yamada, H.; Idogaki, Y.; Ogawa, S.; Suami, T. Total Synthesis of (+)-Asteltoxin1. *Tetrahedron* **1990**, *46*, 2353–2366. [CrossRef]
30. Eom, K.D.; Raman, J.V.; Kim, H.; Cha, J.K. Total Synthesis of (+)-Asteltoxin. *J. Am. Chem. Soc.* **2003**, *125*, 5415–5421. [CrossRef]
31. Schreiber, S.L.; Satake, K. Studies of the Furan-Carbonyl Photocycloaddition Reaction: The Determination of the Absolute Stereostructure of Asteltoxin. *Tetrahedron Lett.* **1986**, *27*, 2575–2578. [CrossRef]
32. Schreiber, S.L. [2 + 2] Photocycloadditions in the Synthesis of Chiral Molecules. *Science* **1985**, *227*, 857–863. [CrossRef] [PubMed]
33. D'Auria, M.; Emanuele, L.; Racioppi, R.; Romaniello, G. The Paterno-Buchi Reaction on Furan Derivatives. *Curr. Org. Chem.* **2003**, *7*, 1443–1459. [CrossRef]
34. Mitani, F.; Lin, J.; Sakamoto, T.; Uehara, R.; Hikita, T.; Yoshida, T.; Setiawan, A.; Arai, M.; Oneyama, C. Asteltoxin Inhibits Extracellular Vesicle Production through AMPK/MTOR-Mediated Activation of Lysosome Function. *Sci. Rep.* **2022**, *12*, 6674. [CrossRef] [PubMed]
35. Salem, M.; El-Metwally, M.; Saber, W.; Negm, S.; El-Kott, A.; Mazroua, Y.; Makhlouf, A.; Moustafa, M. Secondary Antiviral Metabolites from Fungi with Special Reference to Coronaviruses. *BIOCELL* **2022**, *46*, 1979–1988. [CrossRef]
36. Wang, J.; Wei, X.; Qin, X.; Tian, X.; Liao, L.; Li, K.; Zhou, X.; Yang, X.; Wang, F.; Zhang, T.; et al. Antiviral Merosesquiterpenoids Produced by the Antarctic Fungus Aspergillus Ochraceopetaliformis SCSIO 05702. *J. Nat. Prod.* **2016**, *79*, 59–65. [CrossRef] [PubMed]